Synthesis and Characterization of Mesoporous Carbon with Narrow Pore Size Distribution Derived from Rare Earth–Macromolecule Complexes

Yanqiu Li,[1,2] Kaixi Li[1]

[1]*Key Laboratory of Carbon Materials, Institute of Coal Chemistry, Chinese Academy of Sciences, Taiyuan 030001, People's Republic of China*
[2]*Graduate University of Chinese Academy of Sciences, Beijing 100049, People's Republic of China*

Received 2 July 2010; accepted 17 December 2010
DOI 10.1002/app.34010
Published online 12 April 2011 in Wiley Online Library (wileyonlinelibrary.com).

ABSTRACT: Mesoporous carbon with narrow pore size distribution was novelly derived from rare earth–macromolecule complexes, which were formed by the coordination between grafted novolac-type phenolic resin and rare earth ions (Ce^{3+}). The as-made resins or carbons were characterized by infrared spectrum, thermogravimetry, carbon tetrachloride adsorption, nitrogen adsorption, and scanning electron microscope. The results showed that the rare earth–macromolecule complexes were formed successfully, which could promote the dispersion of rare earth elements in the precursor and further control the pore structure and pore size distribution of as-made mesoporous carbon during steam-activation process. The as-made mesoporous carbon exhibited typical mesoporous structure and relatively narrow pore size distribution, and the mesoporosity of it was up to 88%. © 2011 Wiley Periodicals, Inc. J Appl Polym Sci 121: 3466–3474, 2011

Key words: rare earth–macromolecule complexes; novolac-type phenolic resin; mesoporous carbon; catalysis; steam activation

INTRODUCTION

Among various carbon materials, mesoporous carbon with pore size between 2 and 50 nm, which has large surface areas and pore volumes as well as unique framework, is widely used in selective membranes, catalyst supports, biological reactors, sensors, electrochemistry, heat insulators, etc.[1–7] With the development of science and technology, the researches on mesoporous carbon gradually display great scientific meaning and applicable value.

Many researches have been done to synthesize mesoporous carbon, and there is a profound comprehension on it. The conventional methods of synthesis mesoporous carbon mainly include physical and chemical activation method, catalytic activation method by metal or metal–organic complex, polymer aerogel, and so on. However, the mesoporous carbon produced by these methods usually has a wide pore size distribution. To meet the increasing requirements on the control of pore size, various processes and techniques (template method, defluorination of PTFE, carbon aerogels, polymer blends method, selection of specific precursors, and selection of preparation conditions) were proposed to create pores in carbon materials and control their amount and size.[8] Some of the processes, especially template method, seems to be able to satisfy the requirements on the control of pore structure, but their technology still needs some breakthrough to be applied in industrial production.

The catalytic activation method is widely used for its simplicity and efficiency, and it is also suitable for industrial production. So, there are many reports about catalytic activation, mainly relating to transition metals (iron, cobalt, nickel, etc.[9–13]) and alkaline-earth metals (calcium, etc.[14,15]). But only a few studies have dealt with rare earth metals.[13,16–19] For example, Tamai et al.[16,17] first mixed the rare earth organic compounds with pitch and got mesoporous carbon by steam activation, in which the mesoporosity reached up to 70%; Shen et al.[18,19] investigated the catalysis of cerium oxide and yttrium oxide by impregnating method. However, catalytic activation method is comparatively limited in the control of pore structure and pore size distribution due to the present loading methods. Either impregnating or blending method

Correspondence to: K. Li (likx99@yahoo.com).
Contract grant sponsor: International Cooperation project of the Ministry of Science and Technology; contract grant number: 2010DFB90690-4.
Contract grant sponsor: International Cooperation Project of Shanxi Province; contract grant number: 2010081031-2.
Contract grant sponsor: National Nature Science Foundation of China; contract grant number: 51061130536.

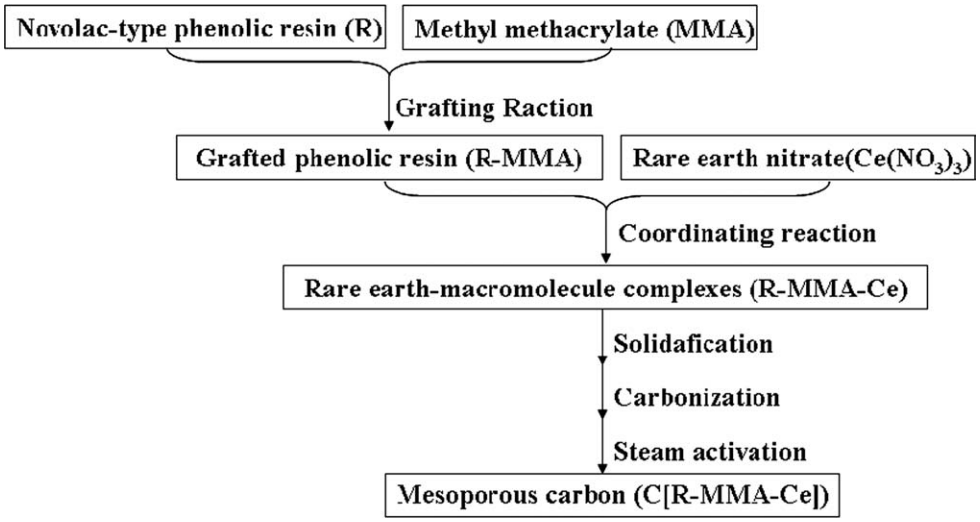

Scheme 1 Illustration of the preparing processes.

belongs to physical doping, so that the dispersion of metal elements in organic precursor cannot reach the level of molecule. And the control of pore structure and pore size distribution was restricted by this heterogeneous dispersion. Consequently, it is necessary to do something to overcome its disadvantage for its future development. And we planed to link the precursor and catalyst by chemical bond to improve the distribution of catalyst.

Rare earth element belongs to hard acid and is easy to coordinate with hard base, and so oxygen is the characteristic coordination atom for rare earth element. Rare earth ion can form complexes with many ligands containing oxygen atom, such as carboxylic acid, β-diketone, and crown ether.[20] Although phenolic resin also has hydroxyl groups, their coordination ability is weaker. Hence, we intended to introduce carboxylic groups into the precursor, namely novolac-type phenolic resin, to increase the opportunity of forming coordination bonds. It was reported that phenol can react with methyl methacrylate (MMA) at the presence of potassium phenolate, in which there exist two reactions simultaneously, namely, the addition reaction on double bond and the transesterification.[21] The two reactions are competitive, and the addition reaction is predominant. Furthermore, Oya et al.[22] had grafted MMA on phenolic resin fiber. Hence, we expected that MMA would be grafted on novolac-type phenolic resin chains by addition reaction, and then the grafted phenolic resin would easily be coordinated with rare earth ions forming rare earth–macromolecule complexes. As shown in Scheme 1, novolac-type phenolic resin first reacted with MMA by the addition reaction of double bonds to form grafted phenolic resin. Then, the grafted ester groups hydrolyzed at basic condition forming carboxylic groups and these groups easily coordinated with rare earth ions creating rare earth–macromolecule complexes. During a series of procedures, namely solidification, carbonization, and steam activation, mesoporous carbon with narrow pore size distribution would be obtained. In detail, the compatibility between organic precursor and inorganic salts would be largely improved by forming coordination bonds, and so the dispersion of rare earth elements would become more homogenous (Scheme 2). This would greatly reduce the phenomenon of agglomeration and improve the catalytic efficiency of rare earth elements. Rare earth ion with high coordination number could bond several oxygen atoms simultaneously connecting near chains together,[20] and so the solidification would be limited owing to the steric effect (Scheme 3). Rare earth elements would be fixed in special areas by forming rare earth–macromolecule complexes. During the following heating process, the coordination bonds easily ruptured forming rare earth oxides,[23] which acted as catalyst during further steam-activation process (Scheme 4).[18] By controlling the activation condition, the rare earth oxides were able to catalyze the assigned location and the neighborhood to realize the aim of controlling pore structure and pore size distribution.

Consequently, this work used rare earth–macromolecule complexes, which were formed by the coordination bond between grafted novolac-type phenolic resin and rare earth ions (Ce^{3+}), to promote the dispersion of rare earth elements in precursor and further to control the pore structure and pore size distribution during steam-activation process. Mesoporous carbon with narrow pore size distribution was obtained and characterized by infrared (IR) spectrum, thermogravimetry (TG), carbon tetrachloride adsorption, nitrogen adsorption, and scanning electron microscope (SEM).

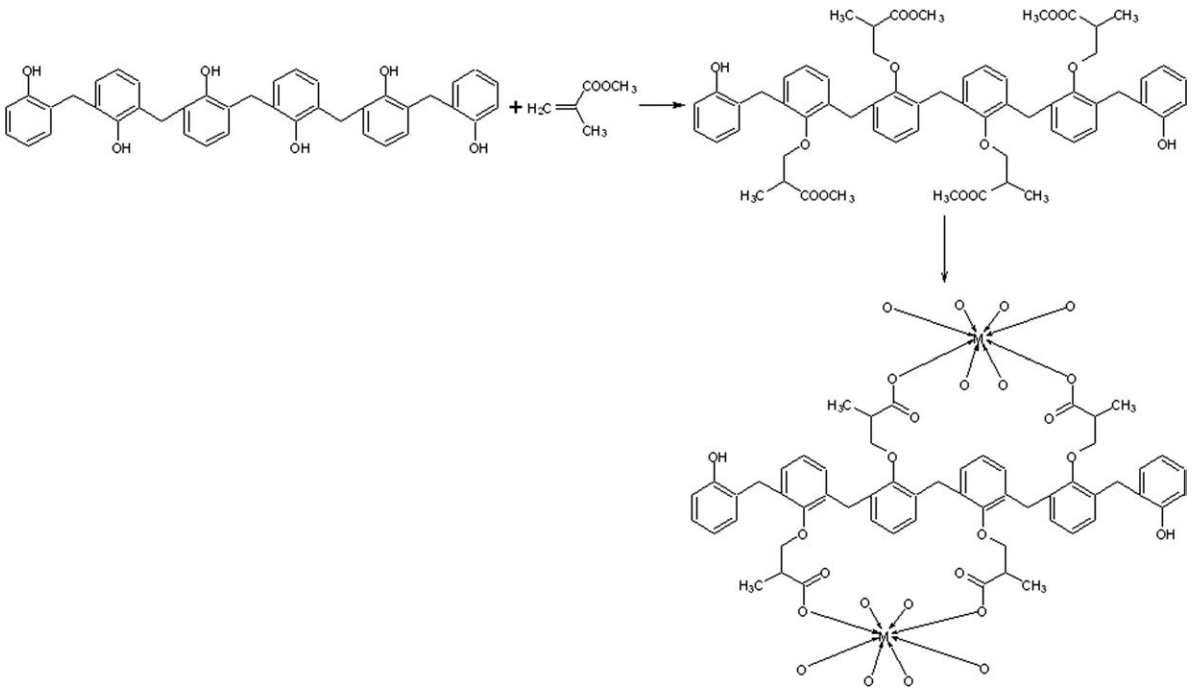

Scheme 2 Illustration of the grafting and coordinating reactions.

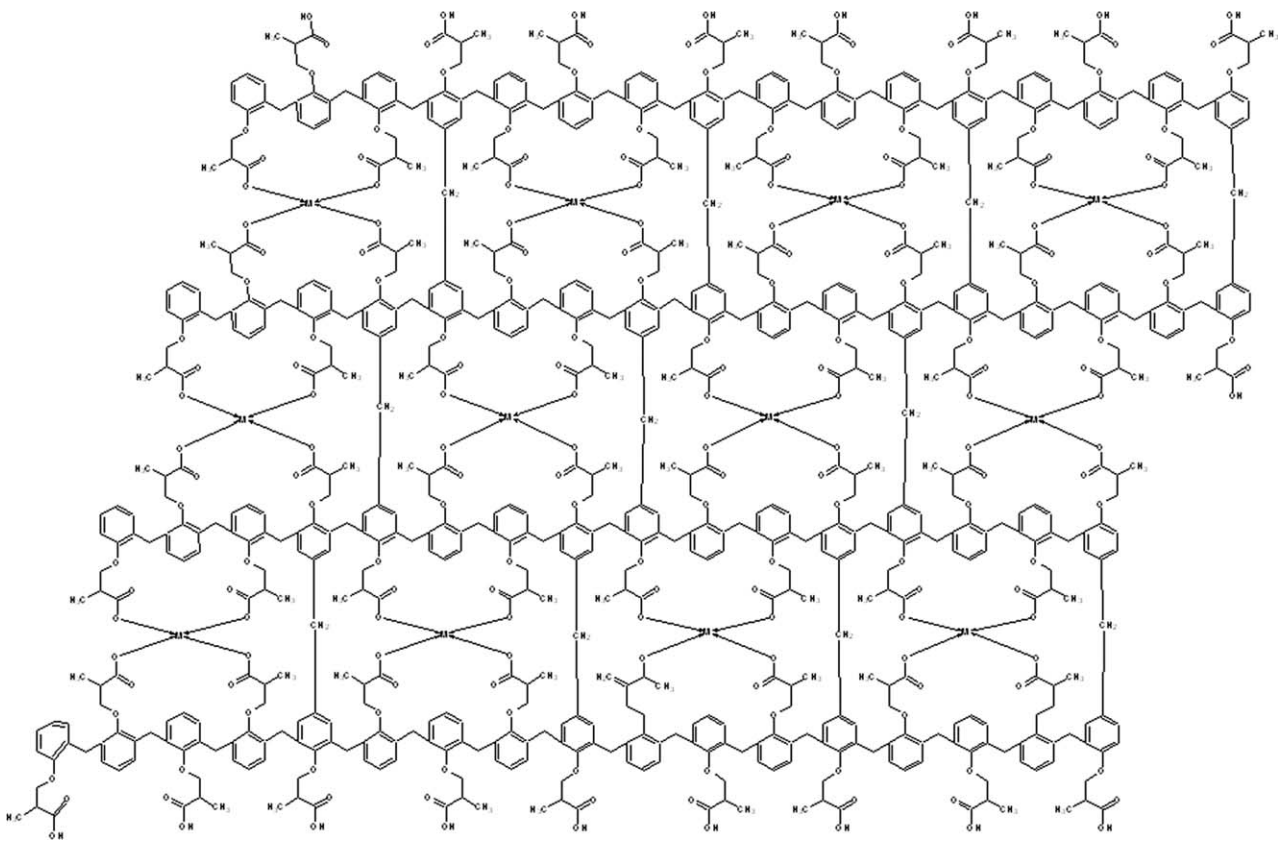

Scheme 3 Illustration of the structure of R-MMA-Ce.

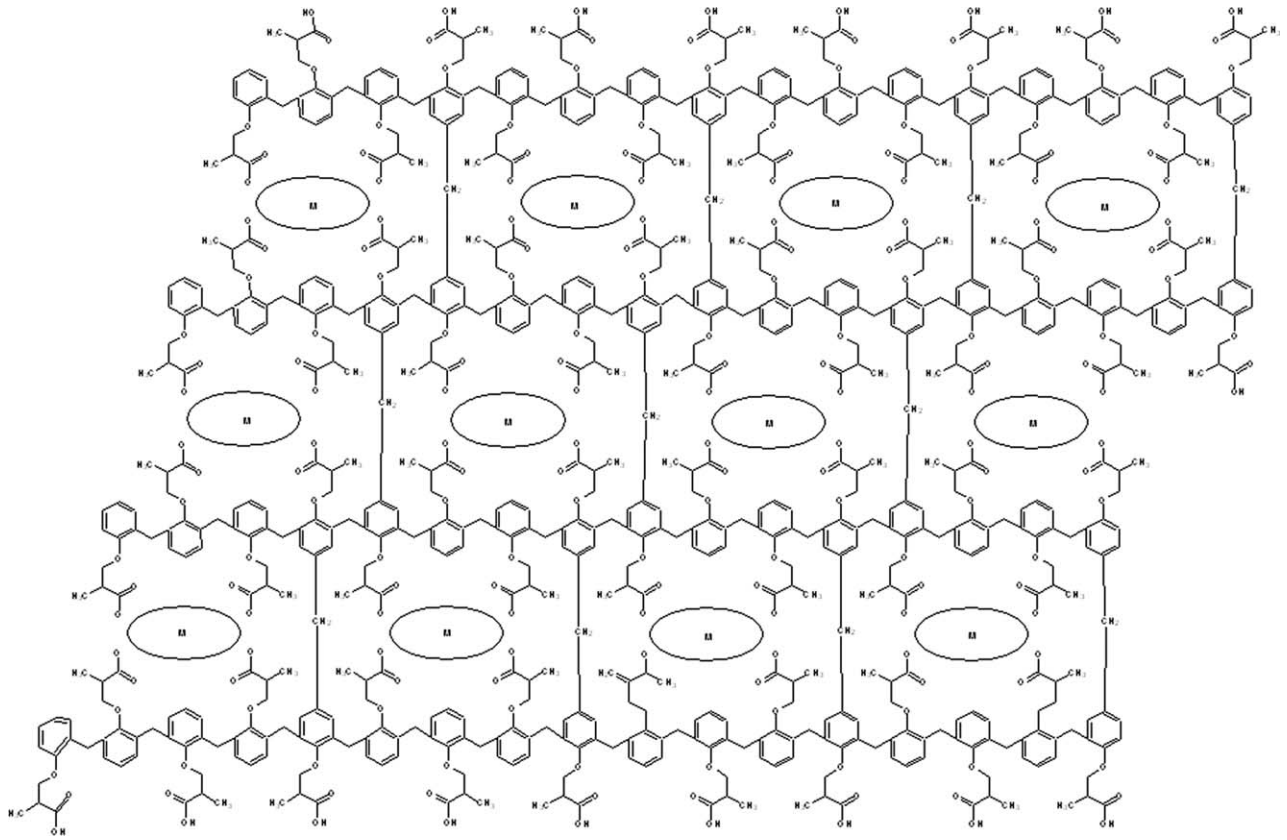

Scheme 4 Illustration of the structure evolution of R-MMA-Ce during heating process.

EXPERIMENTAL

Materials

The novolac-type phenolic resin was a commercially available powder product with a polymerization degree of $\sim$ 500, which was purchased from resin plant in Tianjin and assigned as NO.217. $Ce(NO_3)_3 \bullet 6H_2O$ (A.R.) was imported and distributed by Jinan Henghua Technology Co. MMA (C.P.) was made by Sinopharm Chemical Reagent Co. Potassium hydroxide (KOH, A.R.) was from Tianjin Chemistry Reagent Factory. Ethanol (A.R.) and carbon tetrachloride (CCl_4, A.R.) were produced by Reagent Factory, Tianjin Beichen Founder. All the materials were used as received without any further purification.

Synthesis

In a typical procedure, a 500-mL three-necked round-bottomed flask equipped with a condenser and a mechanical stirrer was charged with novolac-type phenolic resin (10 g) and ethanol (100 mL). The mixture was kept under reflux at 65°C with stirring continuously. MMA (10 mL) and KOH (0.01 g) were added after 0.5 h, and $Ce(NO_3)_3 \bullet 6H_2O$ (0.1 g) was added after another 0.5 h. After additional 6 h, the mixture was filtered, transferred into a dish, and left standing for 1–2 days. The resulting concentrated solution was put into an oven at 100°C for 12 h. And the cured resin (R-MMA-Ce) was scraped from the dish. Then, the resin was calcined in a vertical furnace at 180°C for 1 h and 800°C for 2.5 h under a constant flow of nitrogen with a ramping rate of 2°C/min. In the process, it was activated at 800°C for 1 h with steam. The remainder (C[R-MMA-Ce]) was washed several times with hydrochloric acid to dissolve and remove cerium compounds and then rinsed with hot deionized water until free of chloride ions before drying in air at 110°C overnight.

In addition, for comparison, resin without any addition (R), resin with MMA (R-MMA), and resin with $Ce(NO_3)_3 \bullet 6H_2O$ (R-Ce) were also synthesized as aforementioned process and activated by steam to get the corresponding activated carbon, denoted as C[R], C[R-MMA], and C[R-Ce]. Full characterization and detailed studies of the properties of all synthesized materials were investigated and compared.

Characterizations

IR spectra were collected within the region of 4000–400 cm^{-1} on a Nicolet Fourier spectrophotometer (USA) in solid state using KBr pellet technique. The thermal decomposition behaviors of the samples were monitored using a SDT Q600 V8.2 Build 100 analyzer from room temperature to 1100°C under nitrogen

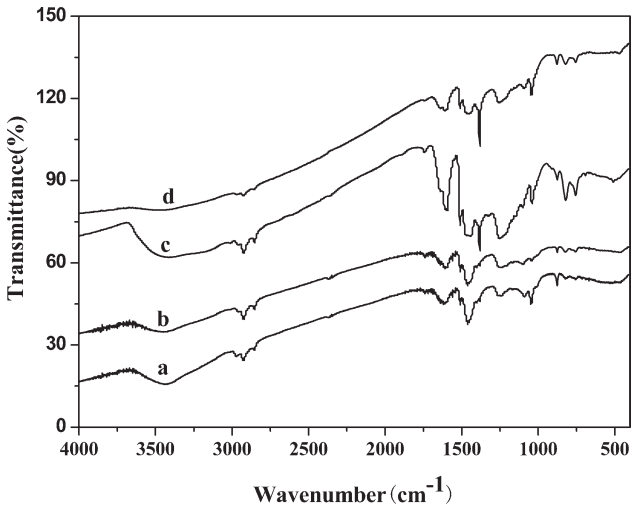

Figure 1 IR spectra of as-made resins: (a) R; (b) R-MMA; (c) R-Ce; (d) R-MMA-Ce.

atmosphere with a heating rate of 10°C/min. The static adsorbed amount of CCl_4 [adsorbed amount of CCl_4 = adsorbed weight of CCl_4 by sample (mg)/ weight of sample (g)] was measured in a desiccator-containing CCl_4 vapor.[24,25] Nitrogen adsorption–desorption isotherms were measured at −196°C on a Quantachrome NOVA 2000e analyzer and a Tristar 3000 sorption analyzer. Before measurements, the samples were degassed in vacuum at 200°C for at least 4 h. The Brunauer–Emmett–Teller (BET) method was used to calculate the specific surface areas. The pore volumes and pore-size distributions were derived from the adsorption branches of isotherms by using the Barrett–Joyner–Halenda (BJH) model.[26–28] The total pore volumes (micropore volume + mesopore volume) were estimated from the liquid volume of nitrogen at a relative pressure of about 0.99. The micropore volumes were calculated from the $V - t$ plot method. The mesopore volumes were obtained by subtracting the micropore volumes from the total pore volumes. The surface morphology of samples was observed on a Hitachi S-5200 field emission SEM.

RESULTS AND DISCUSSION

IR spectra of as-made resins

The infrared (IR) spectra of R, R-MMA, R-Ce, and R-MMA-Ce are shown in Figure 1. After curing, the chains connected together forming 3-D networks structure, and there also existed some free phenols and oligomers in the phenolic resin. So it was difficult to distinguish every peak in the spectra of R. The characteristic peaks of MMA might be covered by the intrinsic peaks of R, and the difference between the spectra of R-MMA and R was not distinct. However, the broad peak at about 3300 cm^{-1} attributing to the stretching vibration of phenolic hydroxyls (υ_{O-H}) and the peak at about 1460 cm^{-1} corresponding to the in-plane bending vibration of phenolic hydroxyls ($\delta_{in\text{-}planeOH}$) became weaker.[29–31] Moreover the peak at 1245 cm^{-1} owing to the symmetric stretching vibration of aromatic ether (υ_{sC-O-C}) became stronger.[29,30] And some small peaks locating at fingerprint region disappeared or appeared. These changes showed that some phenolic hydroxyls were transformed to ether oxygen bonds, indicating that the phenolic resin had reacted with MMA molecules.

In the spectra of R-Ce and R-MMA-Ce, there appeared two new peaks at 1386 and 467 cm^{-1}, respectively. The peak at 1386 cm^{-1} was caused by carboxylic groups,[23,29,31] while the peak at 467 cm^{-1} was attributed to the coordination bonds of Ce—O.[23] The peak at 467 cm^{-1} in the spectrum of R-MMA-Ce was stronger than that in the spectrum of R-Ce, indicating that there appeared more coordination bonds in R-MMA-Ce. In a word, the IR spectra confirmed that the grafting and coordinating reactions were accomplished.

Pyrolysis behavior of as-made resins

Figure 2 represents the weight loss during pyrolysis process of as-made resins. The weight loss was determined from the change in weight between cured resin and final sample. Owing to the condensation of aromatic ribbon molecules and the volatilization of low-molecular weight species, noncarbon elements were removed as volatiles during pyrolysis process. So, the weight loss of R began from 26°C and became significant in the range from 400 to 800°C. The corresponding weight losses of R in the pyrolysis temperature ranges of 26–311°C and 311–1089°C were about 5 and 22%, respectively. Compared to R, the weight of R-MMA lost more

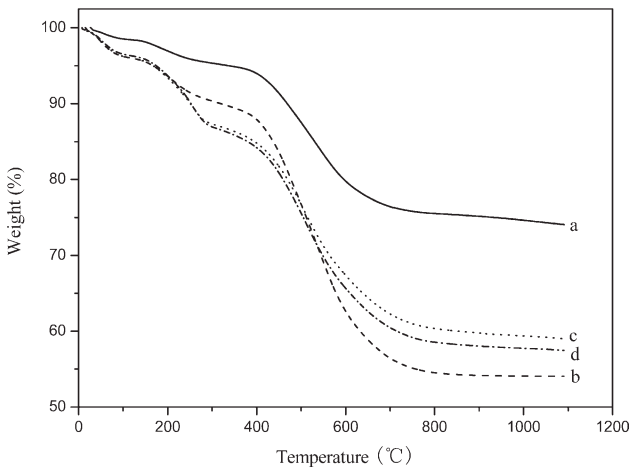

Figure 2 TG curves of as-made resins: (a) R; (b) R-MMA; (c) R-Ce; (d) R-MMA-Ce.

TABLE I
Yield of Activation and Adsorbed Amount of CCl_4

Sample ID	Yield of activation (%)	Adsorbed amount of CCl_4 (mg/g)
C[R]	41	491
C[R-MMA]	40	586
C[R-Ce]	23	855
C[R-MMA-Ce]	30	910

quickly, whose total weight loss was about 47%. The MMA belongs to small molecule and is easier to volatile. Although most of MMA had grafted on the phenolic resin, the formed composition was bonded by ether oxygen bonds and it was not stable.[32] So, the introduction of MMA made the decomposition of phenolic resin more quickly.

The TG curves of R-Ce and R-MMA-Ce lay between that of R and R-MMA, and the total weight loss was 39 and 43% for R-Ce and R-MMA-Ce, respectively. The introduction of $Ce(NO_3)_3$ would increase the pyrolysis rate of phenolic resin, attributing to the catalysis of Ce elements during gasification in the presence of water from $Ce(NO_3)_3 \bullet 6H_2O$.[18] Furthermore, the coordination bonds in the formed complexes not only delayed the gasification for the reinforcement of grafting, but also quicken the decomposition of phenolic resin as a result of the bond cleavage of Ce—O at about 500°C.[23] This synergistic effect made the decomposition of R-MMA-Ce faster than that of R or R-Ce, but slower than that of R-MMA. The phenomenon also reflected that the grafting and coordinating reactions were successful.

Activation yield and adsorption ability of carbons

The activation yield (the weight percentage of the remainder after activation to the cured resin) and adsorption ability of carbons are summarized in Table I. The activation yield and adsorbed amount of CCl_4 for C[R] and C[R-MMA] were similar. However, the activation yield reduced almost by half, and the adsorbed amount of CCl_4 increased to twice when $Ce(NO_3)_3$ was doped. This was attributed to Ce elements, which could accelerate the steam activation and promote the forming of pores.[18]

When the yield was similar, C[R-MMA-Ce] had a larger adsorbed amount of CCl_4, which proved that MMA was grafted on the phenolic resin and formed complexes with Ce^{3+} ions. In detail, if the rare earth–macromolecule complexes were formed, it would make Ce elements disperse more homogenously and further promote the catalytic efficiency of Ce elements, which would be favor for the development of pores.

Pore structure of carbons

Nitrogen adsorption–desorption isotherms and pore size distribution histograms of the carbons are shown in Figures 3 and 4. And the corresponding parameters including BET surface area, pore volume, and pore size are summarized in Table II.

The isotherm of C[R] exhibited a prominent adsorption at low relative pressures and then levered off, which belonged to type I isotherm, indicating the existence of micropores. However, there was also a hysteresis loop of type H4 at the relative pressures from 0.4 to 0.9, which featured parallel and almost horizontal branches, attributing to adsorption–desorption in narrow slitlike mesopores.[33] The adsorption behavior of C[R-MMA] was similar to that of C[R], except that the hysteresis loop was not closed completely. This might be caused by the presence of more micropores in C[R-MMA]. The fast volatilization of free and weekly bonded MMA would leave some smaller pores in the precursor. The isotherm of C[R-MMA-Ce] belonged to Type II isotherm with a hysteresis loop of type H3, in which the isotherm mounted up gradually and did not lever off. This illustrated that there appeared more mesopores in C[R-MMA-Ce] than that in C[R]. Isotherm with Type H3 loop, which did not level off at relative pressure close to the saturation vapor pressure, was reported for materials composed of aggregates (loose assemblages) of platelike particles forming slitlike pores.[33] The isotherm of C[R-Ce] was between Types I and II, and the hysteresis loop was between Type H4 and H3. This made clear that there appeared more mesopores in C[R-MMA-Ce] than that in C[R-Ce], attributing to the formed rare earth–macromolecule complexes.

The pore size distribution of C[R] and C[R-MMA] both showed two weak peaks, illustrating that there

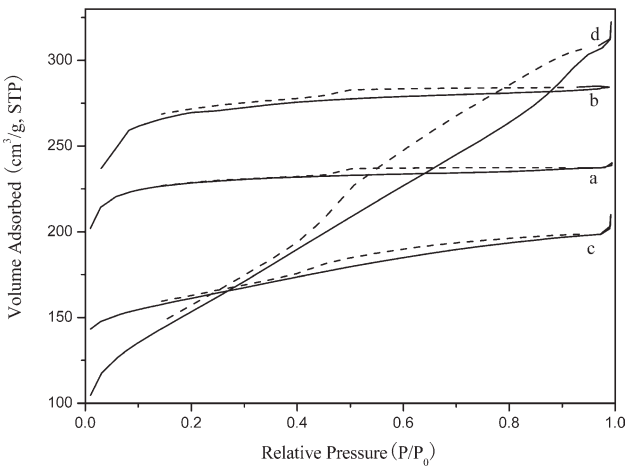

Figure 3 Nitrogen sorption isotherms at −196°C on carbons: (a) C[R]; (b) C[R-MMA], shifted 50 U upward; (c) C[R-Ce], shifted 100 U upward; (d) C[R-MMA-Ce].

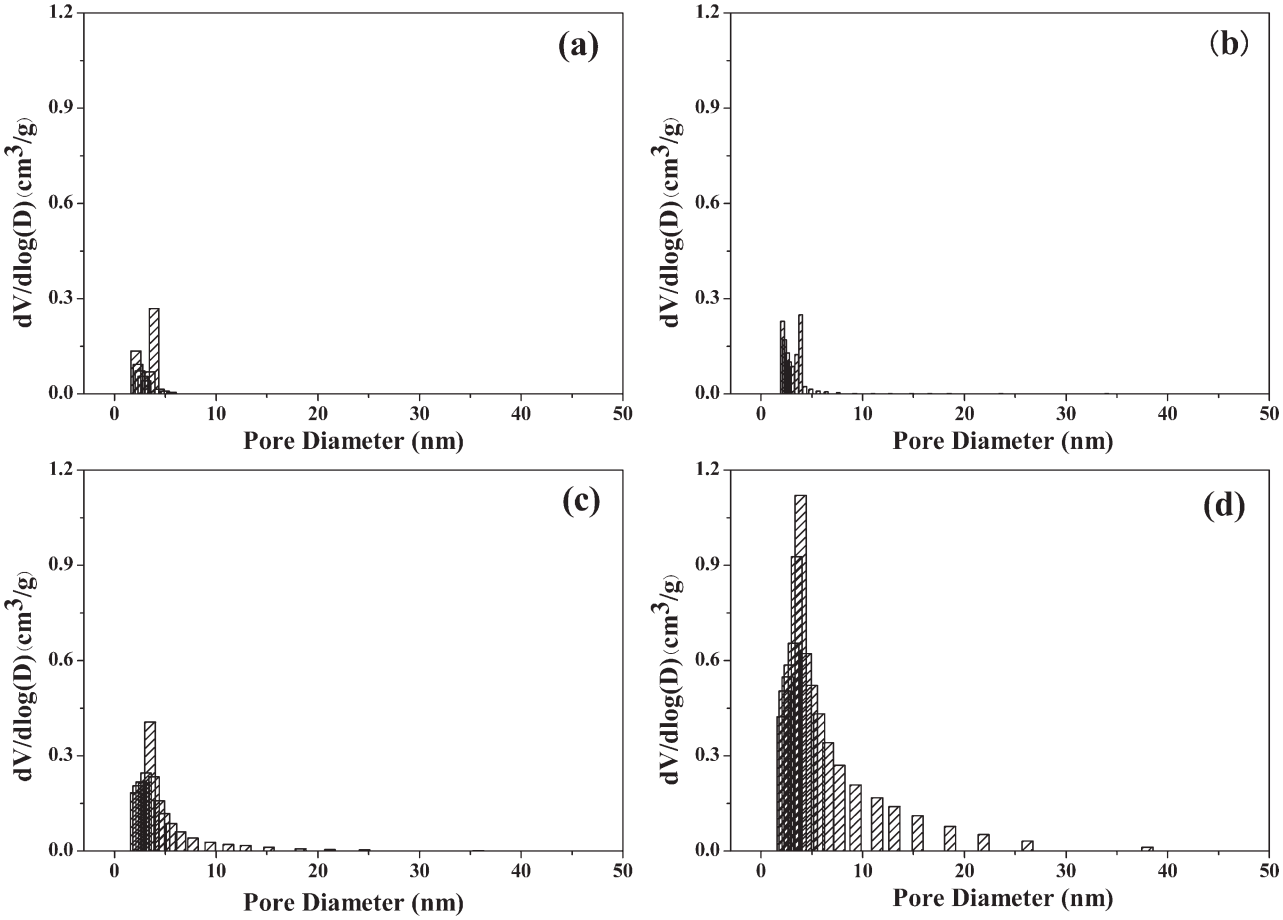

Figure 4 Pore size distribution histograms of carbons: (a) C[R]; (b) C[R-MMA]; (c) C[R-Ce]; (d) C[R-MMA-Ce].

were some micropores and mesopores simultaneously in the two carbons. Although C[R-MMA-Ce] and C[R-Ce] displayed very similar pore size distribution with a peak centering at about 4 nm, the vertex of C[R-MMA-Ce] was much higher. This indicated there appeared an obvious increase of mesopores and a narrow pore size distribution in C[R-MMA-Ce].

BET surface areas were 767, 742, 215, and 541 m^2/g corresponding to C[R], C[R-MMA], C[R-Ce], and C[R-MMA-Ce], respectively. And their corresponding total pore volumes were 0.37, 0.36, 0.27, and 0.60 cm^3/g, respectively. The increase of total pore volume accompanied by the decrease in micropore volume, suggesting an increase of mesopores at the expense of micropores, was similar to the results of Hussein et al.[34] And the mesoporosity (the percentage of mesopore volume to total pore volume, V_{meso}/V_{total}) were 14%, 11%, 82%, and 88%, respectively. When MMA was grafted and rare earth–macromolecule complexes were formed in the precursor resin, the mesoporosity increased enormously from 14 to 88%, which was much higher than that of just doping $Ce(NO_3)_3$ (82%). This phenomenon further

TABLE II
Porosity Parameters of Carbons Calculated from Nitrogen Sorption Isotherms

Sample ID	S_{BET} (m^2/g)	V_{total} (cm^3/g)	V_{micro} (cm^3/g)	V_{meso} (cm^3/g)	V_{meso}/V_{total} (%)	D (nm)
C[R]	767	0.37	0.32	0.05	14	1.94
C[R-MMA]	742	0.36	0.28	0.04	11	1.96
C[R-Ce]	215	0.17	0.03	0.14	82	3.18
C[R-MMA-Ce]	541	0.50	0.06	0.44	88	3.68

S_{BET}, BET surface area; V_{total}, total volume; V_{micro}, micropore volume; V_{meso}, mesopore volume; D, average pore diameter.

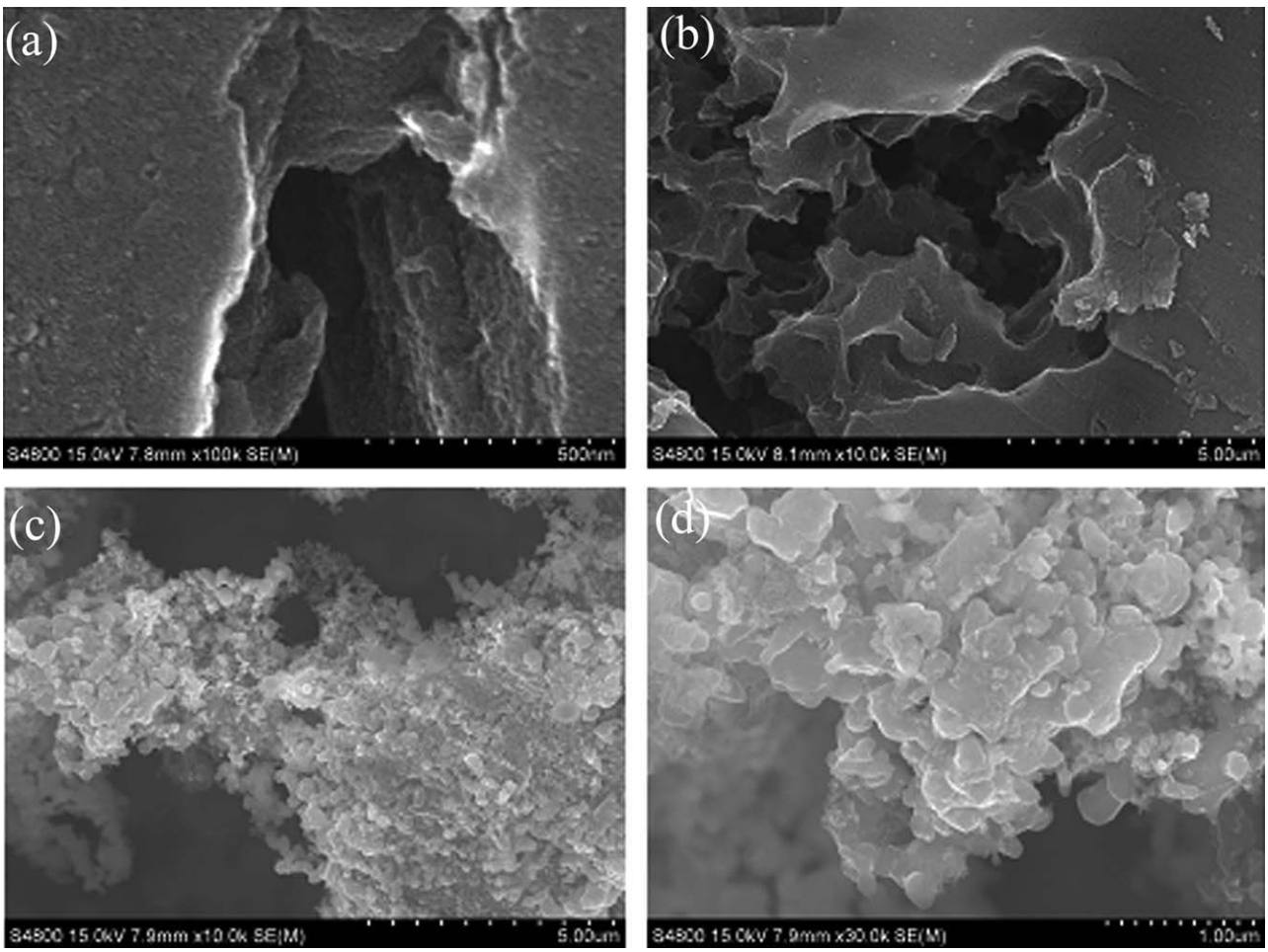

Figure 5 SEM photographs of carbons: (a) C[R]; (b) C[R-Ce]; (c) and (d) C[R-MMA-Ce].

proved that the formed rare earth–macromolecule complexes could improve the dispersion of rare earth elements, boost the efficiency of catalysis, and increase the mesoporosity greatly.

Surface morphology of carbons

The SEM photographs of carbons are shown in Figure 5. C[R] had a comparatively smooth surface and some small holes, indicating the slightly activation by steam. Compared to C[R], the surface of C[R-Ce] was etched much more, and there appeared many cavities irregularly. These may be attributed to the catalysis of Ce elements,[18] the distribution of which was not very homogenous in the precursor resin for the limitation of organic–inorganic compatibility.

The SEM photograph of C[R-MMA-Ce] showed that many small particles seemed loosely assembled together forming aggregate, which was agreed with the results revealed by the nitrogen sorption isotherm. Furthermore, it also displayed that the etching was further deep and uniform. All these demonstrated that the formed rare earth–macromolecule complexes could improve the distribution of Ce elements and further boost the catalytic efficiency of Ce elements.

CONCLUSIONS

In summary, the mesoporous carbon with relatively narrow pore size distribution was obtained by using the novel method of rare earth–macromolecule complexes. On one hand, the formed rare earth–macromolecule complexes could improve the distribution of rare earth elements in precursor resin and boost the catalytic efficiency of rare earth elements. On the other hand, it could also fix rare earth elements in special areas and control the pore structure and pore size distribution to some extent. Although the as-made carbon exhibited not very well in the pore size distribution compared to template method, the present finding provides an example for the development of catalytic activation method to synthesize mesoporous carbon with narrow pore size distribution. A further report will appear soon with respect to optimizing the conditions of synthesis mesoporous carbon with narrower pore size distribution by this novel method.

References

1. Merritt, A.; Rajagopalan, R.; Foley, H. C. Carbon 2007, 45, 1267.
2. Joo, S. H.; Lee, H. I.; You, D. J.; Kwon, K.; Kim, J. H.; Choi, Y. S.; Kang, M.; Kim, J. M.; Pak, C.; Chang, H.; Seung, D. Carbon 2008, 46, 2034.
3. Chavez, V. L.; Song, L.; Barua, S.; Li, X.; Wu, Q.; Zhao, D.; Rege, K.; Vogt, B. D. Acta Biomater 2010, 6, 3035.
4. Zhu, L.; Tian, C.; Zhu, D.; Yang, R. Electroanalysis 2008, 20, 1128.
5. Liu, L.; Meng, Q. H. J Mater Sci 2005, 40, 4105.
6. Lee, J.; Yoon, S.; Hyeon, T.; Oh, S. M.; Kim, K. B. Chem Commun 1999, 21, 2177.
7. Liu, F.; Li, C.; Ren, L.; Meng, X.; Zhang, H.; Xiao, F. S. J Mater Chem 2009, 19, 7921.
8. Inagaki, M. New Carbon Mater 2009, 24, 193.
9. Liu, Z.; Ling, L.; Qiao, W.; Liu, L. Carbon 1999, 37, 663.
10. Oya, A.; Yoshida, S.; Alcaniz-Monge, J.; Linares-Solano, A. Carbon 1995, 33, 1085.
11. Oya, A.; Yoshida, S.; Alcaniz-Monge, J.; Linares-Solano, A. Carbon 1996, 34, 53.
12. Tomita, A.; Higashiyama, K.; Tamai, Y. Fuel 1981, 60, 103.
13. Liu, Z.; Ling, L.; Qiao, W.; Lu, C.; Wu, D.; Liu, L. Carbon 1999, 37, 1333.
14. Leboda, R.; Skubiszewska-Zięba, J.; Bogillo, V. I. Langmuir 1997, 13, 1211.
15. Leboda, R.; Skubiszewska-Zięba, J.; Grzegorczyk, W. Carbon 1998, 36, 417.
16. Tamai, H.; Kakii, T.; Hirota, Y.; Kumamoto, T.; Yasuda, H. Chem Mater 1996, 8, 454.
17. Tamai, H.; Ikeuchi, M.; Kojima, S.; Yasuda, I. Adv Mater 1997, 9, 55.
18. Shen, W.; Zheng, J.; Qin, Z.; Wang, J. J Colloid Interface Sci 2003, 264, 467.
19. Shen, W.; Lu, A.; Zheng, J.; Qin, Z.; Wang, J.; Zhang, Y. J Mater Sci Lett 2003, 22, 635.
20. Huang, C. H. Rare Earth Coordination Chemistry (In Chinese); Science Press: Beijing, 1997.
21. Bieber, P. P. Annal Chim 1954, 12, 674 (In French).
22. Oya, A.; Kimura, M.; Sugo, T.; Katakai, A.; Abe, Y.; Iizuka, T.; Makiyama, N.; Linares-Solano, A.; Lecea C. S. D. Carbon 1994, 32, 107.
23. Ferenc, W.; Walków-Dziewulska, A. Collect Czech Chem Commun 2000, 65, 179.
24. Hakuman, M.; Naono, H. J Colloid Interface Sci 2001, 241, 127.
25. Branton, P. J.; Reynolds, P. A.; Studer, A. Adsorption 1999, 5, 91.
26. Barrett, E. P.; Joyner, L. G.; Halenda, P. P. J Am Chem Soc 1951, 73, 373.
27. Sing, K. S. W.; Everett, D. H.; Haul, R. A. W.; Moscou, L.; Pierotti, R. A.; Rouquerol, J.; Siemieniewska, T. Pure Appl Chem 1985, 57, 603.
28. Ravikovitch, P. I.; Neimark, A. V. Colloid Surf A 2001,187–188,11.
29. Su, K. M.; Pan, T. Y.; Zhang, Y. L. Spectral Analysis Method (in Chinese); East China University of Technology Press: Shanghai, 2002.
30. Poljanîsek, I.; Krajnc, M. Acta Chim Slov 2005, 52, 238.
31. Zoumpoulakis, L.; Simitzis, J. Polym Int 2001, 50, 277.
32. Guo, W.; Chuang, T. H.; Huang, S. T.; Leu, W. T.; Hsiao, S. H. J Polym Res 2007, 14, 401.
33. Kruk, M.; Jaroniec, M. Chem Mater 2001, 13, 3169.
34. Hussein, M. Z.; Tarmizi, R. S. H.; Zainal, Z.; Ibrahim, R.; Badri, M. Carbon 1996, 34, 1447.